



A modified pseudo-steady-state analytical expression for battery modeling

Kudakwashe Chayambuka, Grietus Mulder, Dmitri L. Danilov, and Prof. Peter H. L. Notten*

K. Chayambuka^{a,b,c}, G. Mulder^{a,b}, D.L. Danilov^{c,d} and P.H.L. Notten^{c,d,e}

^a VITO, Boeretang 200, 2400 Mol, Belgium

^b EnergyVille, Thor Park 8310, 3600 Genk, Belgium

^c Eindhoven University of Technology, Postbus 513, 5600 MB Eindhoven, Netherlands

^d Forschungszentrum Jülich (IEK-9), D-52425 Jülich, Germany

^e University of Technology Sydney, Broadway, Sydney, NSW 2007, Australia

* E-mail: p.h.l.notten@tue.nl

Abstract

The solid-state spherical diffusion equation with flux boundary conditions is a standard problem in lithium-ion battery simulations. If finite difference schemes are applied, many nodes across a discretized battery electrode become necessary, in order to reach a good approximation of solution. Such a grid-based approach can be appropriately avoided by implementing analytical methods which reduce the computational load. The pseudo-steady-state (PSS) method is an exact analytical solution method, which provides accurate solid-state concentrations at all current densities. The popularization of the PSS method, in the existing form of expression, is however constrained by a solution convergence problem. In this short communication, a modified PSS (MPSS) expression is presented which provides uniformly convergent solutions at all times. To minimize computational runtime, a fast MPSS (FMPSS) expression is further developed, which is shown to be faster by approximately three orders of magnitude and has a constant time complexity. Using the FMPSS method, uniformly convergent exact solutions are obtained for the solid-state diffusion problem in spherical active particles.

Keywords: *Porous electrodes, Pseudo-steady state, Analytical methods, Spherical diffusion.*

1 Introduction

Efforts to understand internal battery dynamics and to optimize battery designs, rely on fast, accurate, physics-based simulation models. Battery electrodes such as found in nickel metal hydride and lithium-ion batteries are typically porous. These electrodes are based on solid active particles and electron conductive filler materials. The morphology of a porous battery electrode is illustrated in Figure 1a, where a metallic Li anode is separated from a porous cathode attached onto a Cu current collector by a separator. The porous electrode is thus composed of carbon conductive filler (black circles) and active particles (grey circles) while the voids created by the solid particles are occupied by a suitable electrolyte. For simplicity, the polymer binder is not shown.

Electrochemical models of the multi-scale and multi-physics phenomena, inherent to typical porous electrodes, combine thermodynamics, transport phenomena and reaction kinetics at the surface of the active particles [1]. Following Newman's porous electrode theory, a 1D battery model considers the electrolyte and solid particles as two, super-imposed continua [2,3]. Such a model description requires the introduction of a pseudo-2D (P2D) domain, where the diffusion transport processes, occurring within the active particles at a microscopic length scale, are modelled [2,4,5]. Within such a macro-homogeneous, P2D domain, representing discrete particles at different spatial positions across the porous electrode, time dependent concentration profiles of intercalating species are simultaneously resolved. Figure 1b illustrates a P2D layout of a 1D battery model.

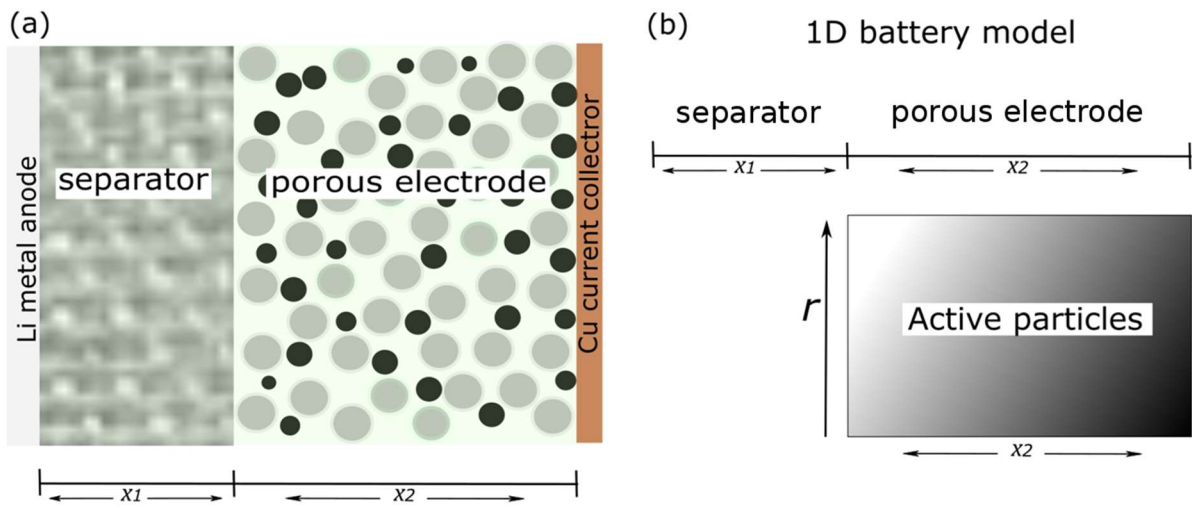


Figure 1. (a) Schematic view of Li-ion battery. (b) Layout of 1D model of a porous electrode showing the active particles in a P2D simulation domain.

P2D porous electrode modeling using numerical methods of finite difference (FDM), finite element (FEM) and finite volume (FVM) is however computationally demanding [3,6,7]. First, by introducing the pseudo radial dimension, the number of mesh nodes in a fully discretized battery model, unavoidably increases. Second, applying explicit finite difference schemes imposes fine time-stepping for numerical stability. Note, however that only the average and surface concentrations are needed to determine the thermodynamic and kinetic properties of the active particles, the rest of concentration profile is not important. This brings about the question whether it is truly necessary to calculate the full concentration profile, if a numerical way to derive these two variables is available. The ‘extra’ pseudo-dimension would therefore be discarded thus reducing the size and computational runtime while maintaining the fidelity of the models.

Several analytical methods have been developed to solve the boundary value problem of spherical diffusion [8–10]. These can be classified as either exact solution methods or

approximate solution methods. Exact solution methods involve a convergent summation of an infinite series of terms which consider the profile history, while approximate solution methods involve empirical approximations and frequently, do not consider the history of the concentration profile. Zhang *et al.* [8] provided a comprehensive review of the different analytical methods relevant to battery simulations. It is therein concluded that the pseudo-steady state (PSS) method and the high-order polynomial method are the leading analytical methods, based on computation speed and accuracy. Incidentally, the former is an exact solution method while the latter is an approximate solution method.

While approximate solution methods generally have speed advantage over either exact solution or numerical methods (*i.e.* FDM, FEM, FVM), they lack the requisite solution accuracy in transient battery simulations; since they do not converge to the exact solution [11]. Existing approximate solution methods include, the low order polynomial method [12], the high order polynomial method [12], the diffusion length method [13,14] and the penetration depth method [15]. On the other hand, exact solution methods offer high accuracy, yet invoke considerable computation effort at short times and whenever the concentration profile undergoes abrupt changes. Exact solution methods have a long and established history, the interested reader is here referred to the seminal works of Carslaw and Jaeger on conduction of heat in solids [16]. Newman's model famously applied Duhamel's superposition integral in the porous electrode theory [2,4,5], while Ölçer's PSS approach, based on the finite integral transform, is rapidly gaining recognition [17,18].

The seemingly antagonistic requirements of speed and accuracy have been resolved by the PSS method, as demonstrated by Liu on a conceptual spherical particle [19]. The PSS method was later applied to a porous electrode model in a benchmarking review by Zhang *et*

al. [8]. Therein, the computational runtime of the PSS emerged of the same order of magnitude as approximate solution methods. However, it has been reported that the PSS method is unstable when the number of summation terms increases [20]. This instability introduces numerical difficulties for control-oriented battery programming [21,22], resulting in few adoptions of the PSS method. In this work, the origins of the numerical problems associated with the PSS method are investigated and addressed resulting in a numerically efficient and stable, modified PSS method (MPSS). Furthermore, a programmable and computationally efficient, fast modified PSS (FMPSS) method is presented for the first time, which enables rapid and accurate porous electrode modeling.

2 Model

Assuming a constant diffusion coefficient, the diffusion controlled transport of intercalated species in a spherical electrode particle is given by the following partial differential equation (PDE)

$$\frac{\partial c}{\partial t} = \frac{D_s}{r^2} \frac{\partial}{\partial r} \left(r^2 \frac{\partial c}{\partial r} \right), \quad (1)$$

where $c = c(r, t)$ is the concentration of the intercalated species in the solid particle [mol m^{-3}], D_s the diffusion coefficient [$\text{m}^2 \text{s}^{-1}$], r the radial distance from the center of the particle [m] and t is time [s]. Figure 2 illustrates the diffusion problem in a spherical particle.

The following Neumann boundary conditions are applied at the surface and center of the spherical particle, respectively:

$$-D_s \frac{\partial c}{\partial r} = j(t), \quad \text{at } r = R_0, \quad t > 0, \quad (2)$$

$$\frac{\partial c}{\partial r} = 0, \text{ at } r = 0, \text{ for } \forall t, \quad (3)$$

where, $\mathbf{j}(t)$ is the flux of species at the surface of the particle [$\text{mol m}^{-2} \text{s}^{-1}$] and R_0 is the radius of the particles [m]. The initial value for the problem of Eq. (1) assumes a constant concentration profile at time $t = 0$, i.e. $c(r, 0) = c_0$, where c_0 is a positive real number.

To solve the set of equations Eq. (1) – (3), finite difference numerical methods can be applied. However, this fundamentally increases the simulation load due to spatial discretization in the particles. Alternatively, one can resort to the PSS analytical method which finds the exact solution, based on established solutions for second order PDEs with flux boundary conditions [17–19].

The PSS analytical expression for Eq. (1) – (3) is

$$\begin{aligned} c(r, t) = & c_0 - \frac{3}{R_0} \int_0^t \mathbf{j}(t) dt + \frac{R_0}{2D} \mathbf{j}(t) \left[\frac{3}{5} - \left(\frac{r}{R_0} \right)^2 \right] \\ & + \frac{2R_0}{D} \sum_{m=1}^{\infty} \frac{\sqrt{1 + \lambda_m^2}}{\lambda_m^3} \frac{\sin\left(\frac{\lambda_m r}{R_0}\right)}{\frac{r}{R_0}} \\ & \times e^{-\frac{\lambda_m^2 D t}{R_0^2}} \left[e^{\frac{\lambda_m^2 D t}{R_0^2}} \mathbf{j}(t) - \frac{\lambda_m^2 D}{R_0^2} \int_0^t e^{\frac{\lambda_m^2 D t}{R_0^2}} \mathbf{j}(t) dt \right], \end{aligned} \quad (4)$$

where λ_m are the non-zero positive real roots of the equation $\tan(\lambda_m) = \lambda_m$ [19]. The infinite summation series in Eq. (4) is truncated when the desired accuracy is obtained.

However, Eq. (4) does not generate stable results at long times irrespective of the number of summation terms. This has been described by Ramadesigan *et al.* [20] as a blow-up of coefficients when summation terms increase. The reason for this instability, is the occurrence of an exponential time function outside the integral term, which results in

oscillatory and non-convergent solutions. As t becomes large, these oscillations become severe, resulting in assured numerical difficulties.

To address this problem, both terms inside the square brackets in Eq. (4) are multiplied by the $e^{-\frac{\lambda_m^2 Dt}{R_0^2}}$ term, resulting in the following MPSS expression

$$\begin{aligned}
c(r, t) = & c_0 - \frac{3}{R_0} \int_0^t \mathbf{j}(\tau) d\tau + \frac{R_0}{2D} \mathbf{j}(t) \left[\frac{3}{5} - \left(\frac{r}{R_0} \right)^2 \right] \\
& + \frac{2R_0}{D} \sum_{m=1}^{\infty} \frac{\sqrt{1 + \lambda_m^2}}{\lambda_m^3} \frac{\sin\left(\frac{\lambda_m r}{R_0}\right)}{\frac{r}{R_0}} \\
& \times \left[\mathbf{j}(t) - \frac{\lambda_m^2 D}{R_0^2} \int_0^t e^{-\frac{\lambda_m^2 D}{R_0^2}(t-\tau)} \mathbf{j}(\tau) d\tau \right].
\end{aligned} \tag{ 5 }$$

Note that separate time symbols t and τ are here introduced. The time at which the solution is calculated is denoted as t , while τ denotes the integration time variable. Thus, in expression $\mathbf{j}(\tau)$, variable τ runs across whole time span of modeling, *i.e.* from 0 to t .

When Eq. (5) instead of Eq. (4) is used to determine the surface concentration, stable and uniformly convergent solutions are obtained for the MPSS. A corresponding test case comparing the PSS and the MPSS is illustrated in Figure 3 when a constant surface flux of $\mathbf{j}(t) = -10^{-3} \text{ mol m}^{-2} \text{ s}^{-1}$ is applied. The negative sign here indicates that the flux is directed towards the center of the particle. Whereas, the PSS has a blow-up of solutions when the number of summation terms goes to infinity, the MPSS method uniformly converges, with greater accuracy at all times. It can therefore be concluded that MPSS represents a stable and accurate implementation of the PSS method.

The MPSS method is however computationally demanding for the long time intervals encountered in porous electrode simulations. As time t increases, a longer time-span has to be integrated. For an efficient programming implementation of Eq. (5), we thus decompose time t to

$$t = t' + \Delta t, \quad (6)$$

where t' is the previous moment of time and Δt is the time step. This relieves the redundancy of integration over previous time steps, whose results are already known. Eq. (5) thus becomes

$$\begin{aligned} c(r, t) = & c_0 - \frac{3}{R_0} \int_0^{t'+\Delta t} \mathbf{j}(\tau) d\tau + \frac{R_0}{2D} \mathbf{j}(t) \left[\frac{3}{5} - \left(\frac{r}{R_0} \right)^2 \right] \\ & + \frac{2R_0}{D} \sum_{m=1}^{\infty} \frac{\sqrt{1 + \lambda_m^2}}{\lambda_m^3} \frac{\sin\left(\frac{\lambda_m r}{R_0}\right)}{\frac{r}{R_0}} \\ & \times \left[\mathbf{j}(t) - \frac{\lambda_m^2 D}{R_0^2} \int_0^{t'+\Delta t} e^{-\frac{\lambda_m^2 D}{R_0^2}(t'+\Delta t-\tau)} \mathbf{j}(\tau) d\tau \right]. \end{aligned} \quad (7)$$

Now, it is necessary to simplify the two integral terms in Eq. (7) and further avoid integration over the whole time span, in order to obtain faster solutions. Denote the convolution integral as a function of roots λ_m and time t as $\chi(\lambda_m, t)$, this leads to

$$\begin{aligned} \chi(\lambda_m, t) = & \int_0^t e^{-\frac{\lambda_m^2 D}{R_0^2}(\tau)} \mathbf{j}(\tau) d\tau = \int_0^{t'+\Delta t} e^{-\frac{\lambda_m^2 D}{R_0^2}(t'+\Delta t-\tau)} \mathbf{j}(\tau) d\tau = \\ & \int_0^{t'} e^{-\frac{\lambda_m^2 D}{R_0^2}(t'+\Delta t-\tau)} \mathbf{j}(\tau) d\tau + \int_{t'}^{t'+\Delta t} e^{-\frac{\lambda_m^2 D}{R_0^2}(t'+\Delta t-\tau)} \mathbf{j}(\tau) d\tau = \end{aligned} \quad (8)$$

$$\chi(\lambda_m, t') + \int_{t'}^{t'+\Delta t} e^{-\frac{\lambda_m^2 D}{R_0^2}(t'+\Delta t-\tau)} \mathbf{j}(\tau) d\tau.$$

The remaining integral on the interval from t' to t can then be evaluated numerically.

Applying trapezoidal integration yields

$$\int_{t'}^{t'+\Delta t} e^{-\frac{\lambda_m^2 D}{R_0^2}(t'+\Delta t-\tau)} \mathbf{j}(\tau) d\tau \approx \frac{\Delta t}{2} \left(e^{-\frac{\lambda_m^2 D}{R_0^2} \Delta t} \mathbf{j}(t') + \mathbf{j}(t) \right), \quad (9)$$

Where the integration error tends to zero as time-step Δt reduces. Substituting Eq. (9) into Eq. (8) produces

$$\chi(\lambda_m, t) = \chi(\lambda_m, t') + \frac{\Delta t}{2} \left(e^{-\frac{\lambda_m^2 D}{R_0^2} \Delta t} \mathbf{j}(t') + \mathbf{j}(t) \right). \quad (10)$$

Indeed, $\chi(\lambda_m, t')$ represents known values from the previous time step while the second term corresponds to the integrand evaluated over Δt .

Now, note that

$$\chi(0, t) = \int_0^t \mathbf{j}(\tau) d\tau, \quad (11)$$

i.e. $\chi(0, t)$ is the time-integrated cumulative flux. Therefore, as a particular case of Eq. (10) one obtains

$$\chi(0, t) = \chi(0, t') + \frac{\Delta t}{2} (\mathbf{j}(t') + \mathbf{j}(t)). \quad (12)$$

This represents an efficient way to calculate the cumulative flux which also enables a rapid determination of the average concentration. From the forgoing derivations, an expression for the FMPSS method is finally obtained

$$\begin{aligned}
c(r, t) = c_0 + \frac{R_0}{2D} \mathbf{j}(t) \left[\frac{3}{5} - \left(\frac{r}{R_0} \right)^2 \right] - \frac{3}{R_0} \chi(0, t) \\
+ \frac{2R_0}{D} \sum_{m=1}^{\infty} \frac{\sqrt{1 + \lambda_m^2}}{\lambda_m^3} \frac{\sin\left(\frac{\lambda_m r}{R_0}\right)}{\frac{r}{R_0}} \left[\mathbf{j}(t) - \frac{\lambda_m^2 D}{R_0^2} \chi(\lambda_m, t) \right].
\end{aligned} \tag{13}$$

Eq. (13), together with iterative relation Eq. (10), represent the FMPSS time-stepping algorithm.

3 Simulation results

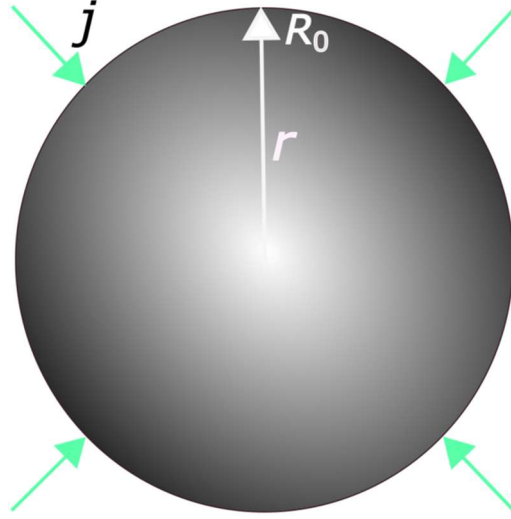


Figure 2. Spherical particle of radius R_0 is used to calculate the analytical surface concentration. \mathbf{j} is the boundary value flux and a color gradient is used to illustrate the concentration profile.

A test case of diffusion in a spherical active particle is herein used to compare the PSS and MPSS behavior. Figure 2 shows a particle undergoing lithiation at a flux \mathbf{j} , while Table 1 lists the parameters used for this calculation. The same parameters were also used by Liu [19].

Table 1. Parameters used in comparing the various analytical expressions.

Parameter	Value	Description
R_0	$3.5 \cdot 10^{-6}$ [m]	Radius of the particle
D	$2.6 \cdot 10^{-10}$ [m ² s ⁻¹]	Diffusion coefficient
Δt	$5 \cdot 10^{-6}$ [s]	Time step
$j(t)$	$-1 \cdot 10^{-3}$ [mol m ⁻² s ⁻¹]	Interfacial boundary flux
c_0	0 [mol m ⁻³]	Initial particle concentration

Figure 3 illustrates the behavior of the PSS (solid lines) and the MPSS (symbols) at four different simulation times ($t = 5, 50, 250$ and $500 \mu\text{s}$) as a function of M , the number of summation terms. Although Eq. (4) and Eq. (5) are both expected to produce identical results, it is evident that the PSS method does not converge to a constant value as time increases. This however, is not the case with the MPSS expression, which requires less terms to reach the solution and is uniformly convergent at all times. The modifications introduced in Eq. (5) therefore allow a stable implementation of the PSS method.

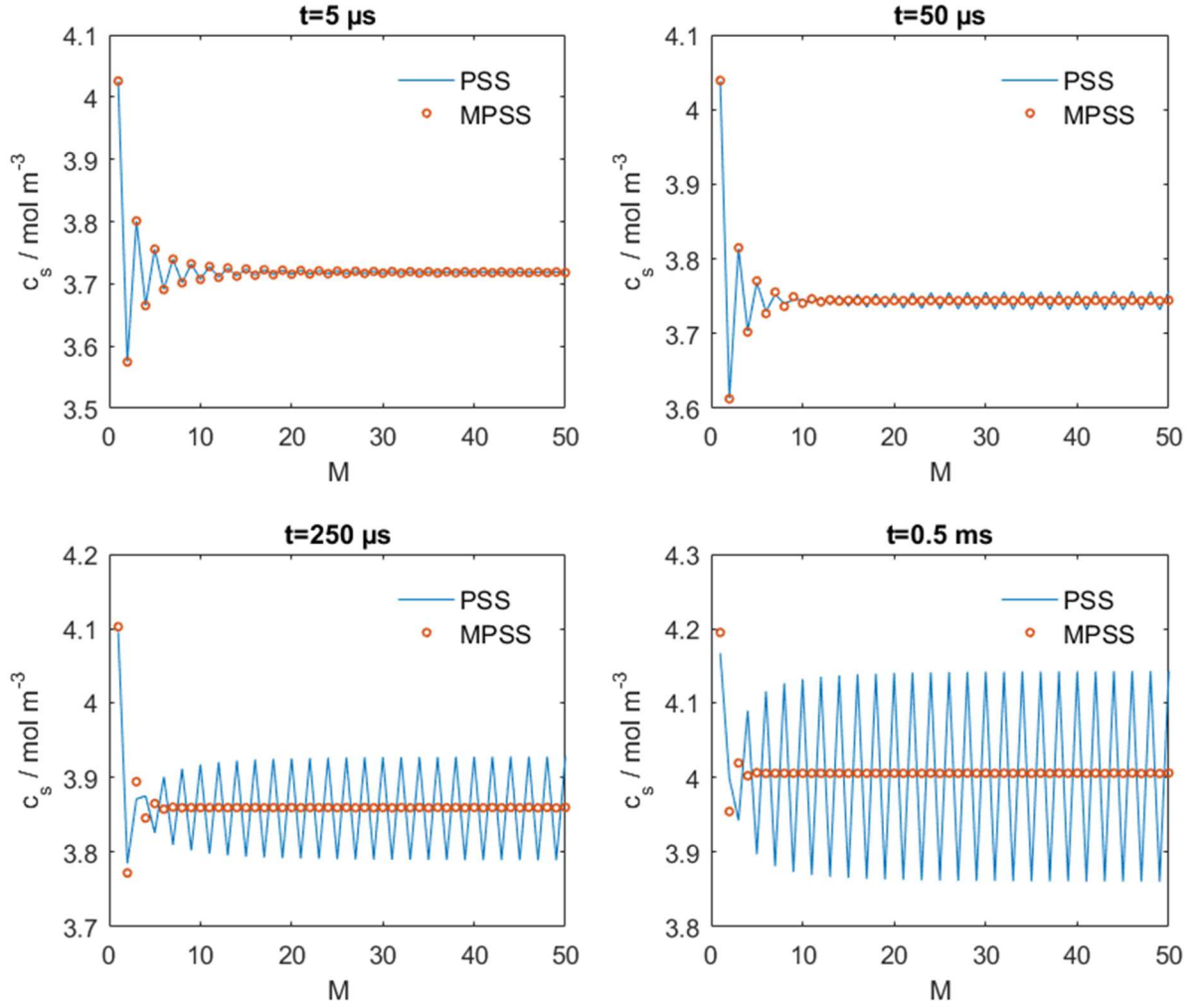


Figure 3. Convergence of the MPSS and PSS methods as a function of M , the number of terms in summation. PSS solutions become oscillatory as time increases while the MPSS method gives uniform convergent solutions at all times.

Nevertheless, the MPSS method is not an efficient way to calculate the surface concentration. As stored data becomes large at long time intervals, integrals from $t = 0$ become cumbersome. Therefore, Eq. (10) and Eq. (13) are programmed as the FMPSS. While similar solutions are obtained using either the MPSS or the FMPSS, significant speed gains are achieved in the latter. Figure 4 illustrates the comparative speed performance between the two methods, as the simulation progresses. Based on these results we observe that the computational runtime per time-step using the FMPSS remains constant while it

evolves linearly for the MPSS method. This implies that the per-step complexity of MPSS is linear with respect to time, *i.e.* $O(t)$, while that of the FMPSS method is constant, *i.e.* $O(1)$. After a simulation time span of 0.05 s, the FMPSS method is shown to be approximately three orders of magnitude faster than MPSS and therefore, a fast and uniformly convergent semi-analytical method.

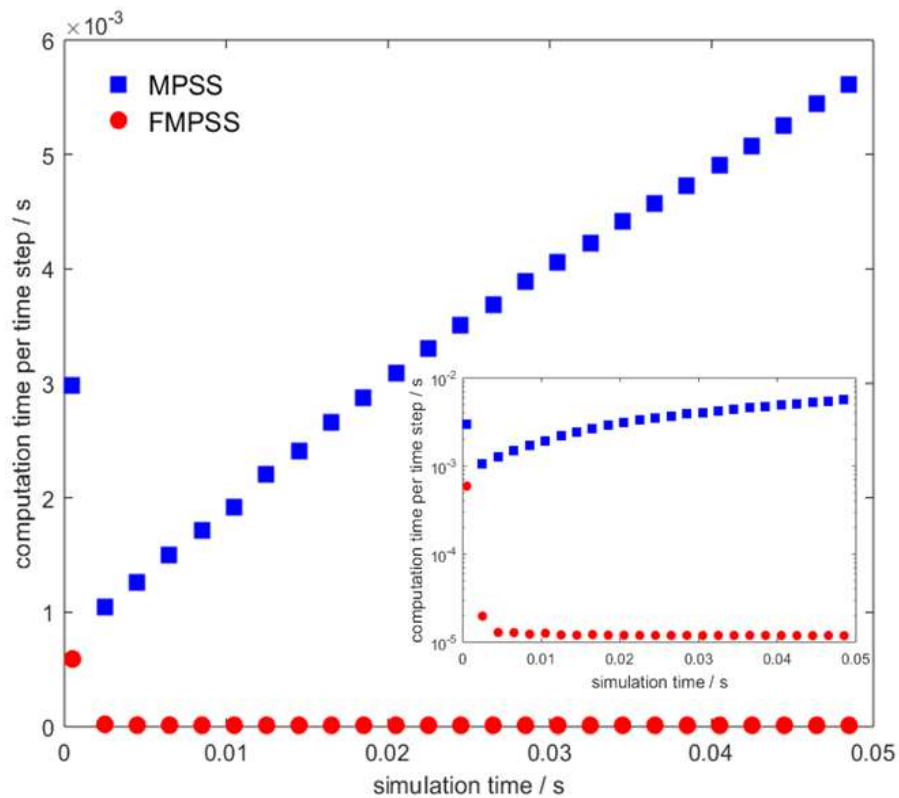


Figure 4. Comparison of computation time using MPSS and FMPSS using parameters listed in Table 1. The results correspond to $M = 40$. Inset showing semi-logarithmic plot of computation time. Approximately three orders of magnitude speed improvement is achieved by the FMPSS method.

4 Conclusions

In the present paper, expedient modifications to overcome solution convergence problems in the pseudo-steady state (PSS) method are elaborated. These modifications result in uniformly convergent and computationally efficient exact analytical solutions to the time

dependent diffusion problem in spherical active particles. The modified PSS (MPPS) expression, herein shown for the first time, produces stable solid-state concentration results at all times. However, the MPSS has a linear time complexity, meaning the computation runtime per time-step increases linearly as the simulation proceeds. Therefore, a fast MPSS (FMPSS) method is introduced which has a constant computation time complexity. Compared to the MPSS, the FMPSS is faster by approximately three orders of magnitude which is ideal for real-time battery modeling application.

The final objective is to implement the FMPSS in a pseudo-2D (P2D) full-cell battery simulation and this will be shown in future work. Within such a P2D model, the FMPSS replaces numerical methods and determines the concentration profile inside the active particles at different spatial positions. It is important however to bear in mind that the PSS, MPSS and FMPSS methods are only valid for a constant diffusion coefficient; a condition which may be violated in phase changing particles. Nevertheless, because the main speed limitation in P2D simulations is due to resolving partial differential equations in the active particles, using the FMPSS method significantly increases the simulation speed. Furthermore, since the FMPSS provides exact analytical solutions, porous electrode battery simulations using this method have enhanced accuracy compared to approximate solution methods. As a result of the accuracy, computational efficiency and solution stability of the FMPSS as demonstrated in this work, this approach should be the leading analytical method for future porous electrode simulations.

Acknowledgements

D.L.D. appreciates support from DEMOBASE project financed by EU HORIZON 2020-GV-2017 program. K.C and G. M are grateful for the support from the European Union's Horizon 2020 Research and Innovation Program under grant agreement No 646433-NAIADES.

References

- [1] J. Newman, K.E. Thomas-Alyea, *Electrochemical systems*, John Wiley & Sons, 2012.
- [2] T.F. Fuller, M. Doyle, J. Newman, Simulation and Optimization of the Dual Lithium Ion Insertion Cell, *J. Electrochem. Soc.* 141 (1994) 1–10.
- [3] R. Zhao, J. Liu, J. Gu, The effects of electrode thickness on the electrochemical and thermal characteristics of lithium ion battery, *Appl. Energ.* 139 (2015) 220–229.
- [4] C.M. Doyle, *Design and Simulation of Lithium Rechargeable Batteries*, Lawrence Berkeley National Laboratory. (1995).
- [5] B. Paxton, J. Newman, Modeling of Nickel/Metal Hydride Batteries, *J. Electrochem. Soc.* 144 (1997) 3818–3831.
- [6] L. Xia, E. Najafi, Z. Li, H.J. Bergveld, M.C.F. Donkers, A computationally efficient implementation of a full and reduced-order electrochemistry-based model for Li-ion batteries, *Appl. Energ.* 208 (2017) 1285–1296.
- [7] L. Zheng, L. Zhang, J. Zhu, G. Wang, J. Jiang, Co-estimation of state-of-charge, capacity and resistance for lithium-ion batteries based on a high-fidelity electrochemical model, *Appl. Energ.* 180 (2016) 424–434.
- [8] Q. Zhang, R.E. White, Comparison of approximate solution methods for the solid phase diffusion equation in a porous electrode model, *J. Power Sources.* 165 (2007) 880–886.
- [9] M. Guo, R.E. White, An approximate solution for solid-phase diffusion in a spherical particle in physics-based Li-ion cell models, *J. Power Sources.* 198 (2012) 322–328.
- [10] V.R. Subramanian, V.D. Diwakar, D. Tapriyal, Efficient Macro-Micro Scale Coupled Modeling of Batteries, *J. Electrochem. Soc.* 152 (2005) A2002–A2008.
- [11] Z. Deng, L. Yang, H. Deng, Y. Cai, D. Li, Polynomial approximation pseudo-two-dimensional battery model for online application in embedded battery management system, *Energy.* 142 (2018) 838–850.
- [12] V.R. Subramanian, J.A. Ritter, R.E. White, Approximate Solutions for Galvanostatic Discharge of Spherical Particles I. Constant Diffusion Coefficient, *J. Electrochem. Soc.* 148 (2001) E444–E449.
- [13] C.Y. Wang, W.B. Gu, B.Y. Liaw, Micro-Macroscopic Coupled Modeling of Batteries and Fuel Cells I. Model Development, *J. Electrochem. Soc.* 145 (1998) 3407–3417.
- [14] C.Y. Wang, V. Srinivasan, Computational battery dynamics (CBD)—electrochemical/thermal coupled modeling and multi-scale modeling, *J. Power Sources.* 110 (2002) 364–376.

- [15] K. Smith, C.-Y. Wang, Solid-state diffusion limitations on pulse operation of a lithium ion cell for hybrid electric vehicles, *J. Power Sources*. 161 (2006) 628–639.
- [16] H.S. Carslaw, J.C. Jaeger, *Conduction of heat in solids*: Oxford Science Publications, Oxford, England, 1959.
- [17] N.Y. Ölçer, On the theory of conductive heat transfer in finite regions, *Int. J. Heat Mass Tran.* 7 (1964) 307–314.
- [18] N.Y. Ölçer, On the theory of conductive heat transfer in finite regions with boundary conditions of the second kind, *Int. J. Heat Mass Tran.* 8 (1965) 529–556.
- [19] S. Liu, An analytical solution to Li/Li⁺ insertion into a porous electrode, *Solid State Ionics*. 177 (2006) 53–58.
- [20] V. Ramadesigan, V. Boovaragavan, J.C. Pirkle, V.R. Subramanian, Efficient Reformulation of Solid-Phase Diffusion in Physics-Based Lithium-Ion Battery Models, *J. Electrochem. Soc.* 157 (2010) A854–A860.
- [21] Z. Chu, X. Feng, L. Lu, J. Li, X. Han, M. Ouyang, Non-destructive fast charging algorithm of lithium-ion batteries based on the control-oriented electrochemical model, *Appl. Energ.* 204 (2017) 1240–1250.
- [22] Y. Zhao, S.-Y. Choe, A highly efficient reduced order electrochemical model for a large format LiMn₂O₄/Carbon polymer battery for real time applications, *Electrochim. Acta*. 164 (2015) 97–107.